



Temperature dynamics and control of a water-cooled fuel cell stack



Daniel O'Keefe ^a, M.Y. El-Sharkh ^b, John C. Telotte ^c, Srinivas Palanki ^{a,*}

^a Department of Chemical & Biomolecular Engineering, University of South Alabama, 150 Jaguar Drive, Mobile, AL 36688-0002, USA

^b Department of Electrical & Computer Engineering, University of South Alabama, 150 Jaguar Drive, Mobile, AL 36688-0002, USA

^c Department of Chemical & Biomedical Engineering, FAMU-FSU College of Engineering, Tallahassee, FL 32310-6046, USA

HIGHLIGHTS

- A model for a water-cooled PEM fuel cell stack was developed.
- A time-varying PID controller was implemented on this model.
- The controller was tested on an experimental power profile from a 3-bedroom house.

ARTICLE INFO

Article history:

Received 13 September 2013

Received in revised form

17 December 2013

Accepted 19 December 2013

Available online 30 December 2013

Keywords:

Water-cooled fuel cell stack

Thermal modeling

PI controller

Stationary power

ABSTRACT

In this paper, a time-varying proportional-integral (PI) controller is designed for controlling the temperature of a water-cooled 5 kW hydrogen fuel cell stack. This controller is designed using a mathematical model for the stack temperature, which is derived using basic chemical engineering material and energy balances. The controller affects the stack temperature by changing the flow rate of cooling water that passes across the stack. The model is then analyzed using a number of power demand profiles to determine the effectiveness of the controller. The results show that a time-varying PI controller is adequate for maintaining the stack temperature within 5 K of the target point.

© 2014 Elsevier B.V. All rights reserved.

1. Introduction

In the search for alternative fuel sources, hydrogen has become a popular option primarily due to the advantages offered by hydrogen fuel cells over the modern internal combustion engine [1]. Fuel cells have multiple advantages over conventional internal combustion engines such as improved efficiency, lack of moving parts, reduced noise during operation and the ability to store energy directly in batteries without any additional steps. Although fuel cells are already readily available for use as backup generators and other stationary power sources, the idea of using a fuel cell for a dynamic power demand is relatively new and the development of such a system is still being researched. One of the biggest concerns in this situation is the ability to keep the fuel cell stack at optimal conditions to maintain the highest efficiency in the face of fluctuating power demand. In the case of a constant power demand, it is much easier to maintain the stack at optimal operating conditions,

but a dynamic power demand requires some reaction to the changes so that the efficiency of the stack can be maintained. In this paper, we focus on the dynamic analysis and control of a water cooled fuel cell stack, which is being used as a backup generator in a stationary environment (e.g. a residential house).

While there have been a large number of papers in the area of modeling fuel cells for different applications, very few of these papers have focused on the issue of temperature dynamics of the fuel cell and its effect on performance. Some of the earliest research into the thermal characteristics of a PEM fuel cell was actually experimental. Amphlett et. al. [2] conducted numerous physical experiments on a working fuel cell stack and determined properties such as the effective mass and surface area of the fuel cell stack. These values compared well with estimates based on bulk stack measurements. The fuel cell stack was also run at various experimental conditions to determine the stack response. These results were then used to experimentally determine further characteristics of the stack including a prediction for the cell voltage, the heat transfer coefficient, and the thermal capacity of the stack. A transient model was also constructed to determine the stack temperature with time, but relies on a large number of inputs that are, at

* Corresponding author.

E-mail address: spalanki@southalabama.edu (S. Palanki).

this point, experimentally determined. Grasser and Rufer [6] developed a thermal model for liquid cooling of a PEM fuel cell in their dynamic model. With their experimental results, they were able to design the thermal model using simple energy balances to express the stack temperature in a first-order differential equation, similar to how Amphlett et al. performed their research.

A variety of theoretical models have been developed to study and model PEM fuel cells. Pukrushpan et al. [12] developed a nonlinear dynamic model that is suitable for control study. Xue et al. [14] developed a dynamic lumped-parameter model of a PEM fuel cell and discovered that hydrogen diffusion through the electrode affects the stack temperature. Pathapati et al. [11] further developed the model set forth by Xue et al. [14] specifically focusing on the dynamics and mechanisms that are of particular importance for automotive purposes. Chu et al. [3] also developed a lumped parameter model, and investigated the changes in stack temperature for various inputs, but control of the stack temperature was not in the scope of their research. Meyer and Yao [9] presented a Multiple Input Single Output (MISO) cooling system model using linearization and μ -synthesis, but this model is again rather complicated and integrated into an overall dynamic model for the stack. Other research has been performed to analyze how the fuel cell stack will perform under adverse conditions, such as starting the stack in freezing temperatures [13].

While various theoretical models have been developed to study the PEM fuel cell stack, they tend to have thermal models developed for a fuel cell stack open to the atmosphere. This air-cooled stack is of interest in the laboratory, but it does not realistically model what the temperature profile of the stack would begin to look like when used in an automobile. When in operation, the atmosphere under the hood of a vehicle can get much hotter than the surrounding environment outside of the vehicle, making the air in the engine compartment unsuitable for adequate cooling of the fuel cell stack. If an air-cooled system is not possible, the only other ways to reliably affect the stack temperature are to modify the inlet conditions or to use a liquid cooling system around the outside of the stack. Since modifications of the inlet conditions will obviously have an adverse effect on the desired power output, a liquid cooling system is the only other feasible option. Significantly less theoretical research has been done on liquid cooling of a fuel cell stack. Recently, Fang et al. [5] developed a dynamic model using a liquid cooling thermal model, but control of the stack temperature was once again not in the scope of their research.

In this research, a theoretical model is developed to model the thermal characteristics of a hydrogen fuel cell stack, as well as its response to changes in parameters that can be used in temperature control. A schematic of the system under consideration is shown in Fig. 1.

The specific objectives are (1) to develop a time-varying proportional-integral (PI) controller for cooling water flow rate across a jacketed PEM fuel cell stack with the intent of controlling the stack

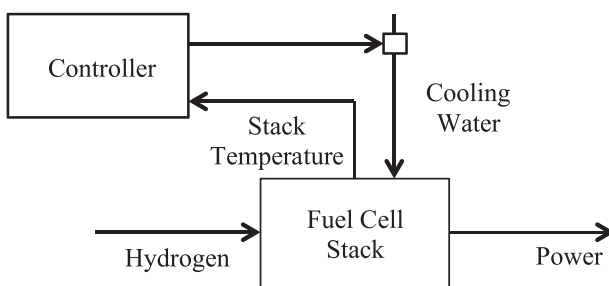


Fig. 1. Basic schematic of fuel cell system.

temperature and (2) test the controller using a variety of power profiles.

Fuel cell stacks currently offer one of the best, cleanest alternatives to the fossil fuels used in modern engines, thereby reducing the amount of harmful greenhouse gases released into the atmosphere. Improvement in the design and efficiency of fuel cell stacks will also make them more affordable for stationary power applications.

2. Development of thermal model

A fundamental premise of the approach taken here is that the electrical characteristics of a fuel cell change much more rapidly than the temperature. A time-scale analysis of this system indicated that the electrical time-scale was of the order of milliseconds, the mechanical flow process time-scale was of the order of seconds and the thermal time-scale was of the order of minutes [8]. Thus we can examine the dynamics of the stack temperature assuming that the voltage adjusts nearly instantaneously when current draw changes. This does not mean that the voltage–current relationship does not depend on temperature, just that the changes occur so rapidly that this part of the overall model can be represented by an algebraic model.

If the fuel cell stack and its contents are chosen as the system, the energy balance can be written as:

$$\frac{dU}{dt} = \sum_i N_{i,in} H_{i,in} - \sum_i N_{i,out} H_{i,out} - \dot{Q} - \dot{W} \quad (1)$$

The material balance for any species i is the following:

$$\frac{dN_i}{dt} = \dot{N}_{i,in} - \dot{N}_{i,out} + \nu_i \dot{\xi} \quad (2)$$

Even though there are separate reactions occurring at the anode and cathode, we combine them into an overall water formation reaction. The accumulation of the species i is very small compared to the mass of the stack. It is therefore safe to assume steady-state for all gaseous and liquid species. This assumption allows the accumulation term in the material balance to be set equal to zero, resulting in:

$$\dot{N}_{i,out} = \dot{N}_{i,in} + \nu_i \dot{\xi} \quad (3)$$

The material and energy balances may now be combined to give:

$$\frac{dU}{dt} = \sum_i \dot{N}_{i,in} (H_{i,in} - H_{i,out}) - \Delta H_{rxn}(T_{out}) \dot{\xi} - \dot{Q} - \dot{W} \quad (4)$$

where the heat of reaction for the overall reaction, the formation of water, will be evaluated at the actual cell outlet temperature. Note that since the $\dot{N}_{i,out}$ term can be written in terms of the $\dot{N}_{i,in}$ term from Eq. (3), the combined equation presented in Eq. (4) is a function of $\dot{N}_{i,in}$ only.

If the hydrogen for the fuel cell is generated by the reforming of a hydrocarbon then the anode inlet flow has hydrogen (H_2), carbon dioxide (CO_2), carbon monoxide (CO) and water (H_2O). The cathode inlet flow is made up of oxygen (O_2), nitrogen (N_2), and water (H_2O). All required species flows can be related to the inlet hydrogen flow. The mole fraction of hydrogen in the inlet is given by:

$$y_{H_2} = \frac{\dot{N}_{H_2,in}}{\dot{N}_{H_2,in} + \dot{N}_{\text{other,in}}} \quad (5)$$

Then all of the other gas flows (carbon dioxide, carbon monoxide, and water) can then be expressed by

$$\dot{N}_{\text{other,in}} = \left(\frac{1 - y_{\text{H}_2}}{y_{\text{H}_2}} \right) \dot{N}_{\text{H}_2,\text{in}} \quad (6)$$

The cathode inlets can similarly be expressed as a function of the hydrogen inlet flow.

$$\dot{N}_{\text{O}_2,\text{in}} = (1 + X_s) \dot{N}_{\text{H}_2,\text{in}} \quad (7)$$

$$\dot{N}_{\text{N}_2,\text{in}} = \frac{79}{21} (1 + X_s) \dot{N}_{\text{H}_2,\text{in}} \quad (8)$$

$$\dot{N}_{\text{H}_2\text{O,in}} = f_s (1 + X_s) \dot{N}_{\text{H}_2,\text{in}} \quad (9)$$

where f_s represents the humidity ratio of the entering air. The previous equations also take into account any excess of oxygen in the system and a cathode stream that is saturated with water. The saturation calculation may be solved or estimated as necessary. This information can now be used to simplify the inlet flow terms of the combined material and energy balance.

$$\sum_i \dot{N}_{i,\text{in}} (H_{i,\text{in}} - H_{i,\text{out}}) = \frac{\dot{\xi}}{X} (T_{\text{in}} - T_{\text{stack}}) C_{p,\text{m}} \quad (10)$$

where

$$C_{p,\text{m}} = C_{p,\text{H}_2} + \left(\frac{1 - y_{\text{H}_2}}{y_{\text{H}_2}} \right) C_{p,\text{CO,CO}_2,\text{H}_2\text{O}} + (1 + X_s) C_{p,\text{O}_2} + \frac{79}{21} (1 + X_s) C_{p,\text{N}_2} + f_s (1 + X_s) C_{p,\text{H}_2\text{O}} \quad (11)$$

and X represents the fractional conversion of hydrogen in the cell and $C_{p,\text{m}}$ is an effective heat capacity for the entering gases. The inlet flow term can further be simplified by setting a constant $\alpha = C_{p,\text{m}}/X$. The inlet flow rate terms can now be expressed as:

$$\sum_i \dot{N}_{i,\text{in}} (H_{i,\text{in}} - H_{i,\text{out}}) = \alpha \dot{\xi} (T_{\text{in}} - T_{\text{st}}) \quad (12)$$

The change in extensive energy term in the combined energy and material balance can also be simplified. It is known that the extensive energy of the system is equal to the sum of the extensive energy of the stack, and the extensive energy of the contents of the stack. It can again be assumed that the mass of the stack makes any change in the contents relatively insignificant when it comes to the stack temperature. The differential term can therefore be approximated as the change in the extensive energy of the stack [2].

$$\frac{dU}{dt} = m_{\text{st}} C_{p,\text{st}} \frac{dT_{\text{st}}}{dt} \quad (13)$$

where m_{st} and $C_{p,\text{st}}$ represent the mass and specific heat of the fuel cell stack. The work term of the combine energy and material balance must be defined. Since the work done by the stack is electrical power, it is only logical to express it as such. The power output for each fuel cell is the product of current draw and voltage. The voltage is a function of current draw, current density, and stack temperature. The total power output for the system is therefore the power output from each cell multiplied by the number of fuel cells in the stack.

$$\dot{W} = n_{\text{cell}} IV_{\text{cell}} \quad (14)$$

where the cell voltage V_{cell} is a function of the current density ($i = I/A_{\text{cell}}$) and the stack temperature (T_{st}) that is represented by the polarization curve. Thus, we can express

$$V_{\text{cell}} = f(I, T_{\text{st}}) \quad (15)$$

where f is a functional form representing the polarization curve. In a fuel cell stack, the polarization curve captures the reduction in voltage with increasing current density due to ohmic and transport resistances and is a function of temperature, pressure and stack material properties. For maximum efficiency, it is desirable to operate at a point in the polarization curve where the power produced is maximum. Thus, a change in stack temperature changes the operating point on the polarization curve. Combining all of these equations, the overall energy and material balance now becomes the following.

$$m_{\text{st}} C_{p,\text{st}} \frac{dT_{\text{st}}}{dt} = \frac{\dot{\xi}}{X} (T_{\text{in}} - T_{\text{st}}) C_{p,\text{m}} - \Delta H_{\text{rxn}} (T_{\text{out}}) \dot{\xi} - \dot{Q} - n_{\text{cells}} IV_{\text{cell}}(I, T_{\text{st}}) \quad (16)$$

The heat of reaction term shown in Eq. (16) must be calculated at the actual operating conditions for the fuel cell stack. This means that it must be evaluated at the stack operating temperature and for the appropriate state (liquid or vapor) of the reaction products. Because we can be in a situation where some of the water formed can be in liquid state, the actual heat of reaction can be calculated from

$$\Delta H_{\text{rxn}} = f_l \Delta H_{\text{rxn,l}} + (1 - f_l) \Delta H_{\text{rxn,v}} = \Delta H_{\text{rxn,v}} - f_l \Delta H_{\text{vap}} \quad (17)$$

where f_l is the fraction of the water formed that exits as a liquid, the subscripts on the heat of reaction terms refer to the values calculated for the water produced as either a vapor or a liquid, and the term ΔH_{vap} is the heat of vaporization of water. To justify neglecting the last term, we should realize that the ratio of the heat of vaporization to the heat of reaction of the vapor is given by:

$$\frac{\Delta H_{\text{vap}}}{\Delta H_{\text{rxn,v}}} = \frac{44}{241.8} = 0.182 \quad (18)$$

This if even as much as 10% of the water exits as a liquid (this would be a very high value), the possible error in using only the heat of reaction to form water vapor (and neglecting the $f_l \Delta H_{\text{vap}}$ term in Eq. (17)) is less than 2%. A more detailed model could incorporate the phase equilibrium calculation that would allow for the calculation of the fraction that exists as a liquid. We hope to address this point in a future publication.

Eq. (16) can be further simplified, however, since the extent of reaction can be related to current draw.

$$I = \beta \dot{\xi} \quad (19)$$

where β denotes the conversion from material flow to current. This can be calculated using Faraday's constant, F , and the number of electrons involved in the reaction, n_e^- . When substituted into the material and energy balance and combining all of the constant parameters into singular constants, the inlet and outlet flow terms can be set as a function of current draw.

$$m_{\text{st}} C_{p,\text{st}} \frac{dT_{\text{st}}}{dt} = C_1 I (T_{\text{in}} - T_{\text{st}}) - C_2 I - \dot{Q} - n_{\text{cells}} IV_{\text{cell}} \quad (20)$$

The constants C_1 and C_2 can be calculated as follows

$$C_1 = \frac{C_{p,\text{m}}}{X n_e^- F} \quad (21)$$

$$C_2 = \frac{\Delta H_{\text{rxn}}}{n_e^- F} \quad (22)$$

Just like the fuel cell stack itself, the cooling water used to regulate the stack temperature has its own dynamics. However, the cooling water temperature is also dependent on position. If the cooling water jacket is divided into n zones, where the temperature within each zone, i , is assumed to be uniform, the energy balance for each zone can be defined as:

$$\frac{dT_i}{dt} = \frac{\dot{m}_{cw}}{\rho V_i} (T_{i-1} - T_i) + \frac{\dot{q}_i}{\rho V_i C_{P_{cw}}} \quad (23)$$

where

$$\dot{q}_i = UA(T_{st} - T_i) \quad (24)$$

This is analogous to considering a plug-flow reactor as a number of CSTRs in series. This simplification results in a model for the cooling water temperature dynamics that is a series of ordinary differential equations. This simplification essentially implies that the stack itself is at a uniform temperature and with this assumption, there is no effect of co-current or counter-current flow. While this "lumped model" approach might not be accurate for a very large stack (e.g. one that supplies 100 kW of power), for a small stack that produces up to 5 kW of power, this is a reasonable approach as shown from the experimental data of Khan and Iqbal [7].

The heat transfer term for the fuel cell stack can be shown to be:

$$\dot{Q} = - \sum_{i=1}^n \dot{q}_i = - \sum_{i=1}^n UA(T_{st} - T_i) \quad (25)$$

This results in the following stack temperature dynamics:

$$m_{st} C_{P_{st}} \frac{dT_{st}}{dt} = \frac{C_{P_{gas}}}{Xn_e F} I(T_{in} - T_{st}) - \frac{\Delta H_{rxn}}{n_e F} I - UA \sum_{i=1}^n (T_{st} - T_i) - n_{cell} IV_{cell} \quad (26)$$

A proportional-integral (PI) controller is modeled in state space as:

$$\dot{m}_{cw} = \dot{m}_{cw,ss} + k_c (T_{sp} - T_{st}) + \frac{k_c}{\tau_I} \int_0^t (T_{sp} - T_{st}) dt \quad (27)$$

where the first term $\dot{m}_{cw,ss}$ is the flow rate of cooling water at steady-state, the second term represents the proportional gain term in the control law and the third term represents the integral term in the control law.

3. Simulation studies

The model developed earlier was simulated in MATLAB. The model parameters used are for a Ballard Mark V 5 kW Fuel Cell stack and are given in Table 1 [7]. It is necessary to parameterize the voltage versus current density relationship in 16 depending on thermodynamic state of the system. This polarization curve is parameterized using the approach proposed by Pukrushpan et al. [12]. A MATLAB program was written to determine the voltage as a function of current, gaseous partial pressures and the temperature at each instance. More details can be found in Ref. [10].

Before performing the calculations, it is first necessary to determine the number of zones that the cooling water channel should be broken into. The number of zones was determined by performing the calculations using various numbers of zones and determining at what point the temperature of the final zone was

Table 1
Parameters from a Ballard Mark V 5 kW fuel cell stack.

Cooling water specific heat, $C_{P_{cw}}$	4.1796 J g ⁻¹ K ⁻¹
Cooling water density, ρ_{cw}	1000 kg m ⁻³
Inlet temperature of cooling water, T_{in}	300 K
Heat transfer parameter for stack, UA_{st}	35.55 + 0.025I W K ⁻¹
Number of cells, n_{cell}	35
Stack length, L	0.38 m
Stack width, W	0.21 m
Cooling water channel thickness, h	0.02 m
Product of stack mass and specific heat, mC_{st}	35 kJ K ⁻¹
Lumped parameter $C_{P_{gas}}/Xn_e F$	1.544 W K ⁻¹ A ⁻¹
Lumped parameter $\Delta H_{rxn}/n_e F$	626.4 W A ⁻¹
Active fuel cell area, A_{cell}	232 cm ²

consistent. There is practically no change in the temperature of the final zone when more than 15 zones are considered, so 15 zones were used in this simulation study.

The first term in the PI controller design equation is the cooling water flow rate needed to keep the stack at the optimal temperature. The literature shows that the target operating temperature for a PEM fuel cell is about 350 K [1]. The difficulty arises, however, in considering the fact that the needed cooling water flow rate is dependent on the current draw; greater current draws will result in greater power output, but also greater heat produced. This additional heat must be removed from the stack to maintain its temperature at the target value.

The first task is therefore to determine the relationship between the current draw and the cooling water flow rate to maintain the stack temperature at 350 K. This was done by considering the same model used for calculating the stack dynamics and setting the stack temperature as constant. It is then possible to perform the calculations for a series of current draws and determine the necessary cooling water flow rate. The needed cooling water flow rates for an inlet cooling water temperature of 300 K are plotted in Fig. 2.

A time-varying PI controller was designed with the goal of minimizing the change in stack temperature from the optimal point. In quantitative terms, the goal was to develop a controller that would keep the stack temperature within 5 K of the target point. The model was given a number of current draw profiles to test the controllers ability to react.

The parameters used to define the PI controller are given in Table 2. These parameters were determined by first considering their proper order of magnitude such that the first term was the major contributor to the steady-state value of the cooling water

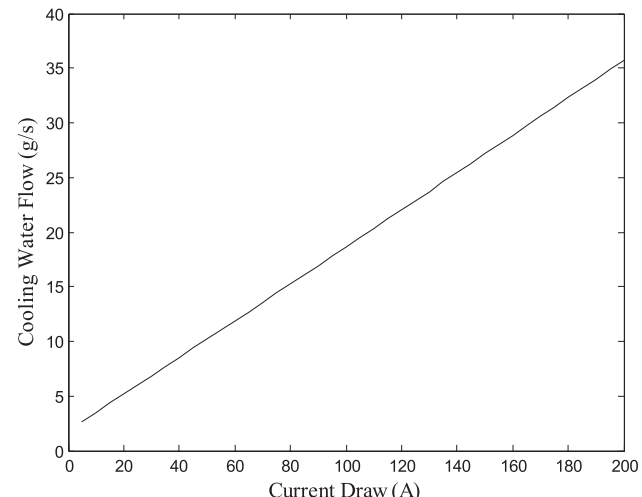


Fig. 2. Cooling water flow rate to achieve stack temperature of 350 K.

Table 2
PI controller parameters.

Set point, T_{sp}	350 K
Steady state water flow rate, $\dot{m}_{cw,ss}$	2–36 g s ⁻¹
Controller gain, k_c	$-0.03 \text{ g s}^{-1} \text{ K}^{-1}$ $I < 25 \text{ A}$ $-0.02 \text{ g s}^{-1} \text{ K}^{-1}$ $I \geq 25 \text{ A}$
Integral time constant, τ_i	75 s $I < 25 \text{ A}$ 125 s $I \geq 25 \text{ A}$

flow rate. The constants were then adjusted using a guess-and-check method until the results of the model had been optimized. The values for these parameters were then used to attempt to control the stack temperature for other current draw profiles.

It was determined that a different set of controller constants was more effective for low current draws where the stack is operating in a non-linear portion of the polarization curve. This is due to a combination of the polarization curve being non-linear and the small changes needed in the cooling water flow rates compared to the changes for larger current draws. The needed cooling water flow rate for current draws below 20 A is very small compared to the flow rate needed for larger current draws, meaning that when the current draw changes, the controller makes much smaller changes to the flow rate than it does when the current draw is

greater. The controller constants are therefore adjusted so that the second and third terms are more effective at adjusting the steady-state flow rate.

Fig. 3 shows a linear current draw (the simplest current draw profile considered) and the effect of the PI controller on the stack temperature for this current draw profile for a constant cooling water flow rate of 5 g s⁻¹, for comparison. **Fig. 3** shows that the controller is extremely effective at maintaining the stack temperature under such simple demands, with virtually no change in the stack temperature from the optimal value. The plots of the corresponding cooling water flow rate and temperature are shown **Fig. 4**.

Further analysis of the results does reveal that the stack temperature begins to stray at the high end of the current draw profile, suggesting that the controller has difficulty in properly adjusting the cooling water flow rate. Considering the controller model and the correlation between the current draw and necessary cooling water flow rate, it would be expected that the controller performance would degrade when the second and third terms were too small. If the adjustments made to the flow rate were too small, then the stack temperature would be expected to rise, which is exactly the result seen. This breakdown begins to occur at a current draw of about 280 A, which is beyond the applicability of the polarization curve correlation.

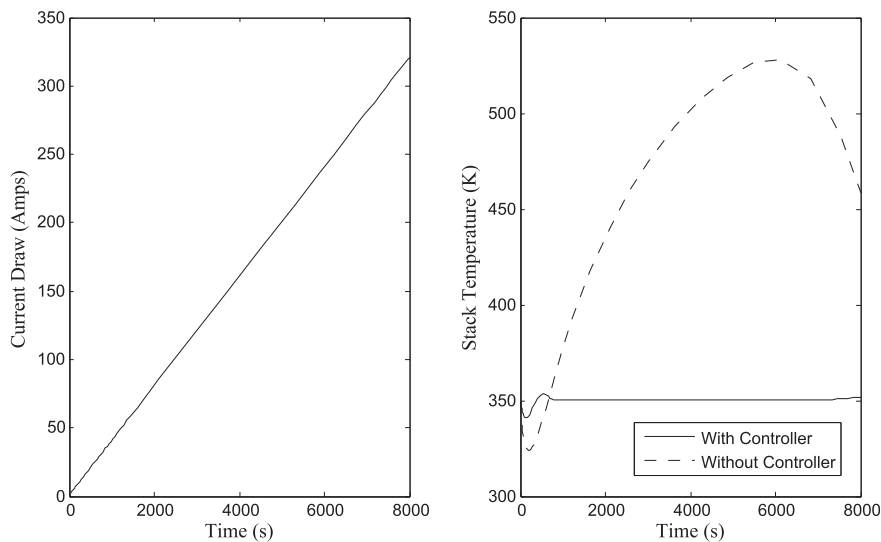


Fig. 3. Stack dynamics for linear current draw.

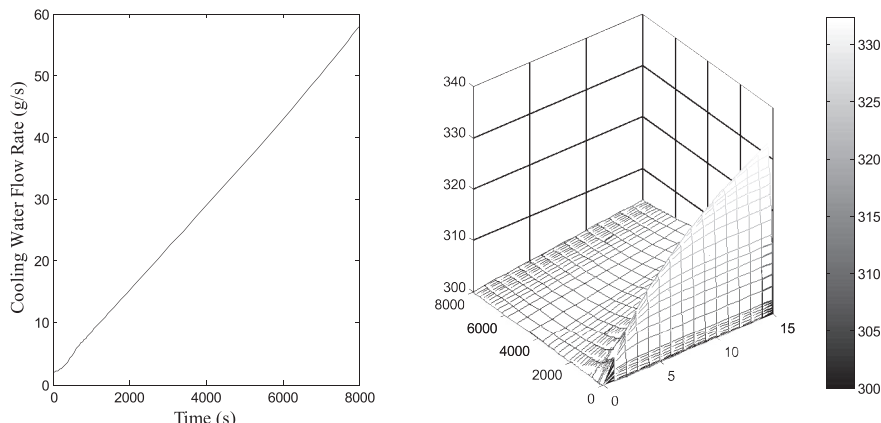
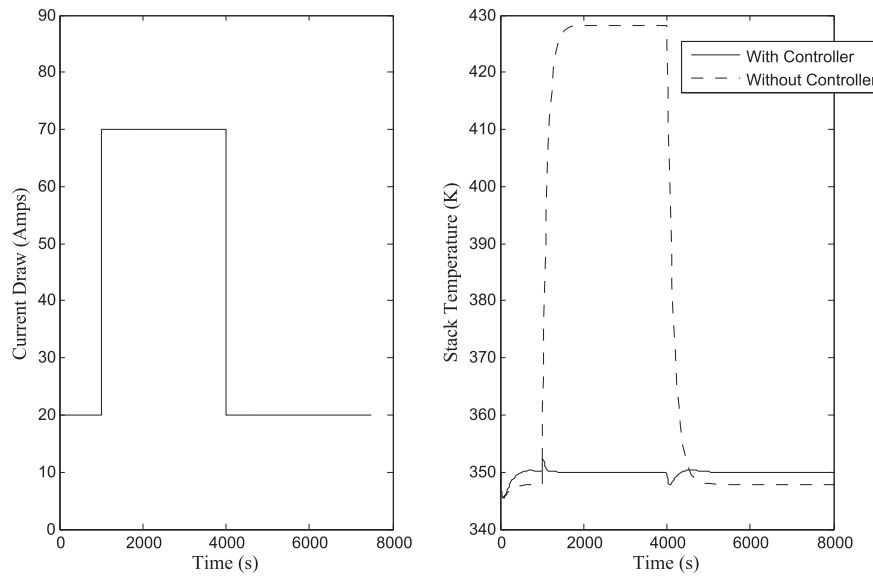
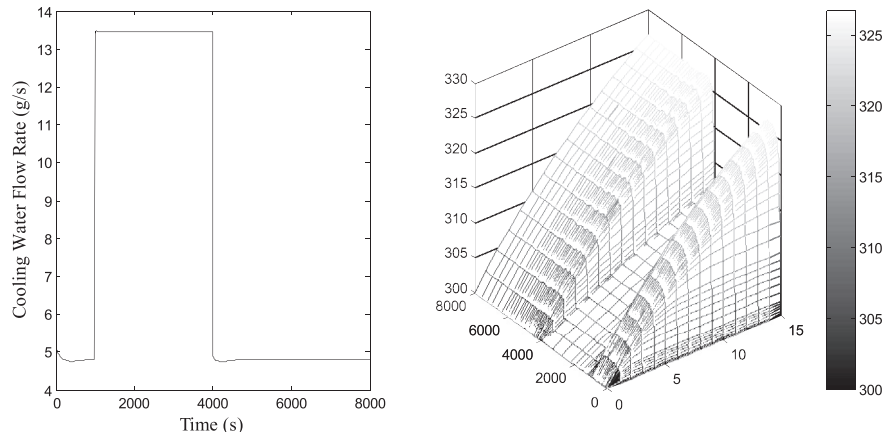
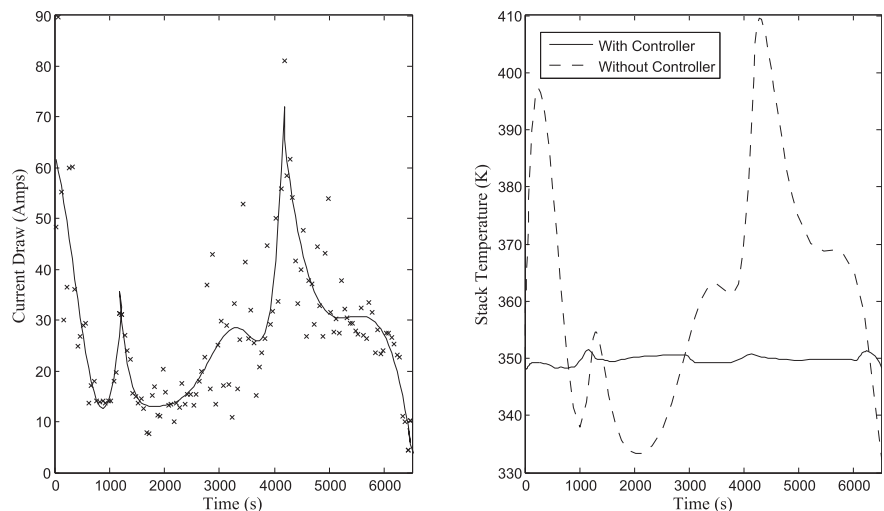


Fig. 4. Cooling water dynamics for linear current draw.

**Fig. 5.** Stack dynamics for pulse function current draw.**Fig. 6.** Cooling water dynamics for pulse function current draw.**Fig. 7.** Stack dynamics for high current draw.

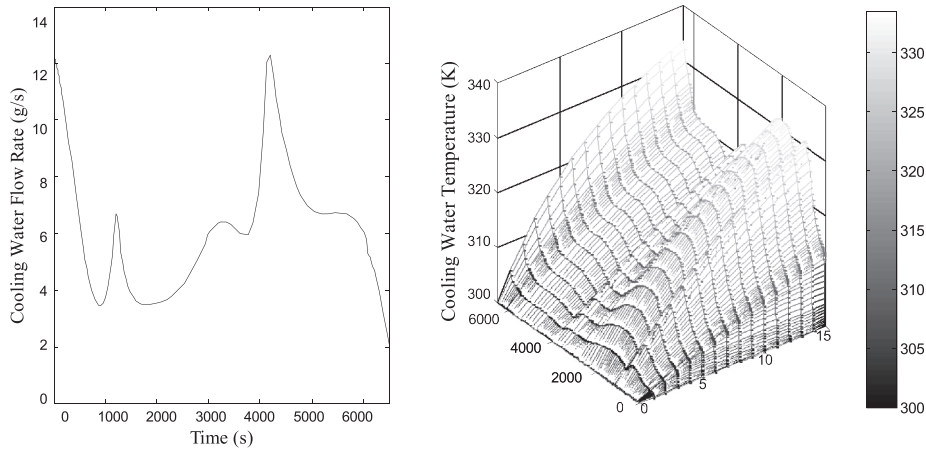


Fig. 8. Cooling water dynamics for high current draw.

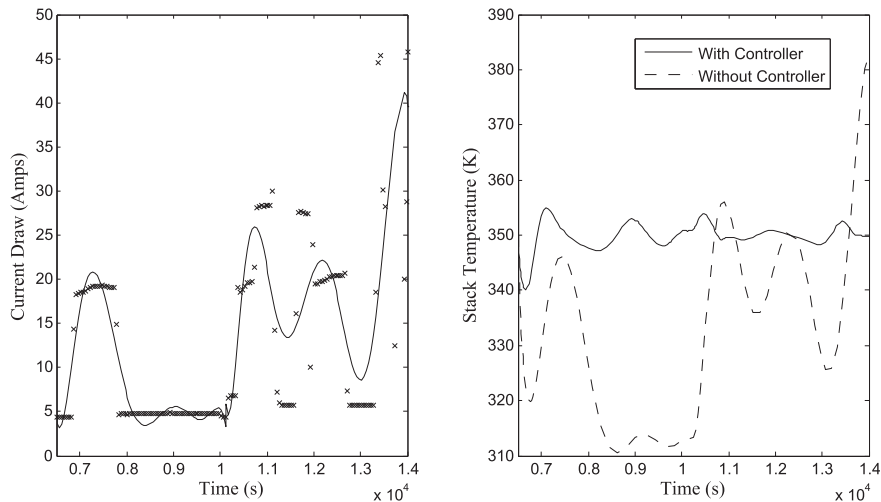


Fig. 9. Stack dynamics for low current draw.

The next simple current profile considered is that of a pulse function. In this case, it is possible to examine the ability of the controller to react to large, sudden changes in the current draw. Sudden changes such as this are fairly common in many real world applications, so it is vital that the controller be able to quickly and effectively respond. The results of this model are given in Figs. 5 and 6, and demonstrate that the designed controller is very effective at

handling isolated step changes. The stack temperature shows a visible controller response within about 50 s of each disturbance, allowing the stack temperature to change by only about 2.5 K before returning to the target temperature in each case. That corresponds to a 97% reduction in the change in stack temperature from the reference case of constant cooling water flow. Fig. 6 also provides the best example of the PI controller at work. At $t = 4000$ s,

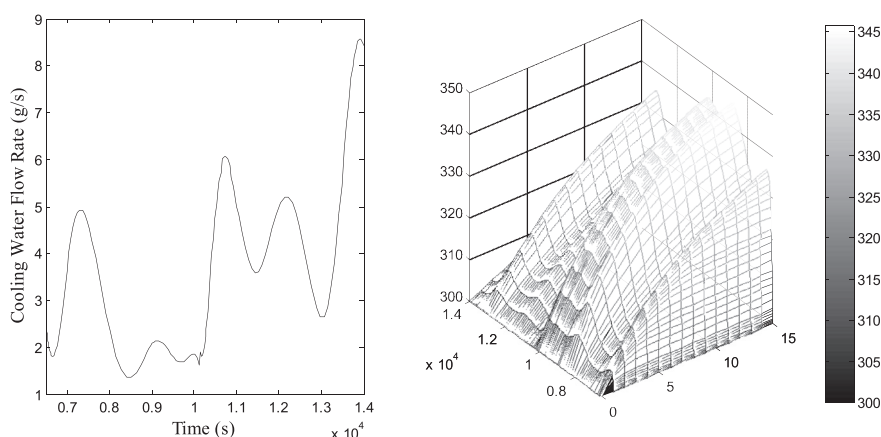


Fig. 10. Cooling water dynamics for low current draw.

there is a step change in the current draw. This step change causes the controller to suddenly change the cooling water flow rate for two reasons; the first reason is simply the difference in the steady-state cooling water flow, which is the first term in Eq. (26). The controller also accounts for the deviation in the stack temperature from the set point, which explains the small changes in the cooling water flow rate for about 500 s following the step change in current draw.

The model was tested using two current profiles obtained from experimental data from a 3 bedroom house [4]. The experimental data was broken into two current profiles, each with a different trend. The first profile considers the current draw on a home during peak hours, so the profile has multiple drastic changes in the power demand. The second profile considers the power demand in non-peak hours, featuring sections of time with little change in the current draw. The results for the first current profile based on experimental data are given in Figs. 7 and 8.

The results show that the controller greatly reduces the resulting changes in stack temperature. The greatest deviation in stack temperature is only about 1.5 K; by comparison, the greatest deviation in stack temperature from the average temperature in the model without the controller is approximately 41 K. That means if the model without the controller was designed to operate at its average stack temperature (368 K), then the maximum deviation from the ideal temperature would be about 41 K. Comparing the controller deviation in stack temperature to this best case scenario model without a controller gives a 96.5% reduction in the variation of stack temperature. The average outlet temperature of the cooling water is around 320 K, with a maximum outlet temperature of 333 K. This maximum change in the cooling water temperature could prove problematic for a system with recycled cooling water, but not for a system where the water is disposed or used for other purposes.

The second current profile from experimental data is designed using the same procedure as the first. Figs. 9 and 10 show the current profile and the results from the calculations. The results show that the controller is notably less effective, mainly because the average current draw for the second profile is much lower than 20 A. The maximum deviation from 350 K is just under 5 K and the deviations average about 2 K. Using the same comparison as in the previous current draw profile, the average operating temperature for the reference model without the controller is approximately 335 K, and the maximum deviation from this temperature is 48 K. This means that the controller still reduces the deviation in stack temperature by as much as 96%. Although the controller is certainly less effective at lower current draws, it still achieves the desired result within the given restraints. The required cooling flow rates are not excessive in any of the simulations and it is not necessary to use chilled water.

4. Conclusions

A dynamic model of a water cooled fuel cell stack was developed and simulated in conjunction with a state space model of a PI controller. The stack temperature dynamics and cooling water temperature dynamics models were linked and solved simultaneously, while all other dynamics inside the fuel cell were considered to operate at pseudo-steady-state. A time-varying PI controller was designed for the theoretical model of a PEM fuel cell stack jacketed by cooling water. The controller adjusts the cooling water flow rate through the jacket to maintain the stack temperature at an optimal operating point. The model was tested using multiple power profiles, including two power profiles obtained experimentally from a residential house. It was determined that the controller is capable of maintaining the stack temperature within 2 K for most current draws, and within 5 K for current draws below 20 A.

References

- [1] Fuel Cell Handbook, fifth ed., U.S. Department of Energy, Morgantown, WV, 2000.
- [2] J. Amphlett, R. Mann, B. Peppley, P. Roberge, A. Rodrigues, *J. Power Sources* 61 (1996) 183–188.
- [3] K. Chu, J. Ryu, M. Sunwoo, *J. Power Sources* 171 (2007) 412–423.
- [4] M. El-Sharkh, A. Rahman, M. Alam, P. Byrne, A. Sakla, T. Thomas, *J. Power Sources* 138 (2004) 199–204.
- [5] L. Fang, D. Li, R. Yang, A Dynamic Model of PEM Fuel Cell Stack System for Real Time Simulation, School of Mechanical Engineering, South China University of Technology, Guangzhou, China, 2009.
- [6] Felix Grasser, Alfred C. Rufer, A Fully Analytical PEM Fuel Cell System Model for Control Applications, Laboratoire d'Electronique Industrielle, Ecole Polytechnique Fédrale de Lausanne, Switzerland, 2007.
- [7] M. Khan, M. Iqbal, *Fuel Cells* 4 (2005) 463–475.
- [8] P. Kolavennu, J.C. Telotte, S. Palanki, *Int. J. Hydrogen Energy* 34 (2009) 380–387.
- [9] R.T. Meyer, B. Yao, in: 2006 ASME International Mechanical Engineering Congress and Exposition. IMECE2006–14151, ASME, Chicago, IL, 2006.
- [10] D.B. O'Keefe, Temperature Dynamics and Control of Fuel Cell Systems, M.S. thesis, University of South Alabama, 2012.
- [11] P. Pathapati, X. Xue, J. Tang, *Renew. Energy* 30 (2005) 1–22.
- [12] J.T. Pukrushpan, A.G. Stefanopoulou, H. Peng, *Proc. Am. Control Conf.* (2002).
- [13] M. Sundaresan, R. Moore, *J. Power Sources* 145 (2005) 534–545.
- [14] X. Xue, J. Tang, A. Smirnova, R. England, N. Sammes, *J. Power Sources* 133 (2004) 188–204.

Notation

English letters

- A_{cell} : active fuel cell area, m^2
 A_{cs} : reactor cross sectional area, m^3
 C_1 : lumped parameter, $\text{W K}^{-1} \text{A}^{-1}$
 C_2 : lumped parameter, W A^{-1}
 C_p : specific heat, $\text{J mol}^{-1} \text{K}^{-1}$
 CV : conversion factor
 D_p : catalyst particle diameter, m
 f_s : saturation calculation
 F : Faraday's constant, C mol^{-1}
 G : superficial mass velocity, $\text{kg m}^{-2} \text{s}^{-1}$
 h : cooling water channel height, m
 H : molar enthalpy, J mol^{-1}
 ΔH_{298} : standard heat of reaction, kJ mol^{-1}
 ΔH_{rxn} : molar heat of reaction, J mol^{-1}
 i : current density, A m^{-2}
 I : current, A
 k_c : controller proportional constant, $\text{kg s}^{-1} \text{K}^{-1}$
 L : fuel cell stack length, m
 m : mass, kg
 m : mass flow rate, kg s^{-1}
 n_{cell} : number of cells in stack
 n_e : number of electrons
 N : molar flow rate, fuel cell stack, mol s^{-1}
 p : partial pressure, kPa
 P : pressure, kPa
 q : molar flow rate, reactor, mol s^{-1}
 Q : heat flow into reactor per unit volume, W m^{-3}
 Q : heat flow, W
 r : reaction rate, $\text{mol s}^{-1} \text{m}^{-3}$
 R : universal gas constant, $\text{J mol}^{-1} \text{K}^{-1}$
 T : temperature, K
 U : internal energy, J
 UA : heat transfer parameter, W K^{-1}
 V : reactor volume, m^3
 V_{cell} : cell voltage, V
 V_n : volume per cooling water zone, m^3
 W : fuel cell stack width, m
 W : work flow, W
 X : fractional conversion of primary reactant
 X_e : fractional excess oxygen fed to fuel cell stack
 y : gaseous mole fraction

Greek letters

- ϵ : efficiency factor
 μ : viscosity, $\text{kg m}^{-1} \text{s}^{-1}$
 μ : stoichiometric ratio
 ξ : extent of reaction, mol s^{-1}
 ρ : density, kg m^{-3}

τ_1 : transfer function dimensionless parameter
 τ_2 : transfer function dimensionless parameter
 τ_i : controller integral constant, s
 ϕ : void fraction of catalyst in reformer

Subscripts

c: catalyst
cw: cooling water

CO_2 : carbon dioxide
 C_2H_5OH : ethanol
 H_2 : hydrogen
 H_2O : water
in: inlet condition
out: outlet condition
sp: set point
st: stack
T: total sum of chemical components in reactor